Reducing effects from environmental temperature on the natural frequencies of tensegrity structures

Nasseradeen Ashwear*, Anders Eriksson

KTH Mechanics, Royal Institute of Technology
Osquars backe 18, SE-100 44 Stockholm, Sweden

Abstract

In vibration health monitoring, dynamic properties such as natural frequencies and mode shapes are used as tools for assessing the structures health condition. They are, however, also affected by environmental conditions like wind, humidity and temperature changes. Of particular importance is the change of the environmental temperature, and it is the most commonly considered environmental variable that influences the vibration health monitoring algorithms. This paper discusses how the tensegrity structures can be designed such that some of their lowest natural frequencies are less sensitive to the temperature changes. A genetic algorithm is used to solve the optimization problem. In the form-finding stage, an asymmetric self-stress vector can be chosen so that the criterion is fulfilled as well as possible. The level of pre-stress can also be regulated to achieve the solution, particularly when a symmetric self-stress vector is chosen.

Keywords: Tensegrity, Self-stress, Temperature effects, Optimization, Structure health monitoring, Vibration health monitoring

*Corresponding author. Tel +4687906184
Email address: ashwear@mech.kth.se (Nasseradeen Ashwear)

1. Introduction

Tensegrities are inherently non-linear cable-strut assemblies which find their stiffness and self-equilibrium states from the integrity between tension and compression. Their stiffness can be improved by regulating the level of pre-stress, using their lowest natural frequencies as indicators for their pre-stress [1]. In vibration health monitoring ('VHM'), the lowest natural frequencies are used as indicators of damage presence [2]. It is well known that, the sensitivity of the natural frequencies to damage is the core of VHM. However, the natural frequencies are also affected by environmental conditions like wind, humidity and temperature changes. Of particular importance is the change of the environmental temperature, and this is the most commonly considered environmental variable influencing the VHM algorithms [3, 4].

To avoid confusion when interpreting the results from VHM algorithms, there are two options: a prior understanding and knowledge of the behaviour of the healthy structure with temperature changes, or optimizing the design of the structure such that its natural frequencies are very little sensitive to the temperature changes. Most of the studies found in literature show that an increase in temperature leads to a decrease in structural frequencies. Xia et al. [5] reviewed the effect of temperature on vibration properties of civil structures and gave some case studies. They concluded that an increase in temperature leads to a decrease in natural frequencies due to reduced pre-stressed stiffness. Their conclusion is in agreement with other studies regarding the relation between the temperature changes and natural frequencies. However, this is not necessarily the case for pre-stressed structures such as tensegrity structures [4].

In [4] we have investigated the influence of temperature changes on the natural frequencies of tensegrity structures, and concluded that, the temperature changes highly influence the natural frequencies. In this paper we investigate how a tensegrity structure can be optimized such that its lowest natural frequencies have a very low sensitivity to the temperature changes.

The effect of temperature changes on the natural frequencies depends on the material used for components, support conditions and the size and shape of the tensegrity structure [4]. In general, the temperature variations change the natural frequency through the change in size (expansion coefficients) and the change in the elastic modulus.

In literature, optimization problems for tensegrity structures are normally classified into size, shape and topology optimization [6]. However, the optimum solution here was achieved by finding the internal force distribution (self-stress vector), which keeps one natural frequency unchanged with temperature changes for a certain (pre-decided) topology, shape, and size of the tensegrity structure. Two methods have been used to achieve the optimum design:

- Using a symmetric self-stress vector, where in this case the level of prestress is regulated such that the natural frequencies are not affected by temperature changes. This method has been explained considering a simple 2D string and tube assembly shown in Fig. 1 and a 3D T3 tensegrity prism, Fig. 2(b).

- Using an asymmetric self-stress vector where the internal force distribution in each module is regulated until the natural frequencies of the structure become approximately non-affected from temperature change. This was explained and implemented on a 3D T3 tensegrity

prism, Fig. 2(b).

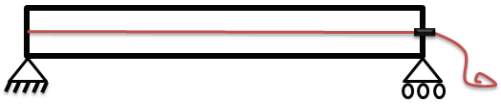

Fig. 1 String and tube assembly

2. Formulation strategy

In the first method, for complex structures like the T3 tensegrity prism shown in Fig. 2(b), a feasible symmetric unit self-stress vector $\hat{\boldsymbol{g}}$ is chosen by means of one of the Form-Finding methods available in literature. For simple structures like the tube and string shown in Fig. 1 this can be done by inspection. Then, this unit self-stress vector can be scaled to regulate the level of pre-stress by means of the scaler ψ. Hence, the self stress vector will be seen as:

$$\boldsymbol{g} = \psi \hat{\boldsymbol{g}}, \tag{1}$$

where ψ is the level of pre-stress and $\hat{\boldsymbol{g}}$ represents the force density coefficients in each component of the structure. In other words, $\hat{\boldsymbol{g}}$ represents the internal force distribution pattern in the whole structure. In this method, the level of pre-stress represented by ψ is the optimization variable.

When using the second method, the equilibrium matrix $\boldsymbol{A}$ is evaluated in the Form-Finding stage from a given topology and nodal coordinates for one single module, the 'base module'. A singular value decomposition (SVD) of $\boldsymbol{A}$ gives the numbers of mechanisms m and independent self-stress states s, respectively. However, in this study the support conditions were applied such that the number of self-stress states $s = 1$, and one infinitesimal mechanism $m = 1$ existed. For this case, the unilateral conditions (tension for

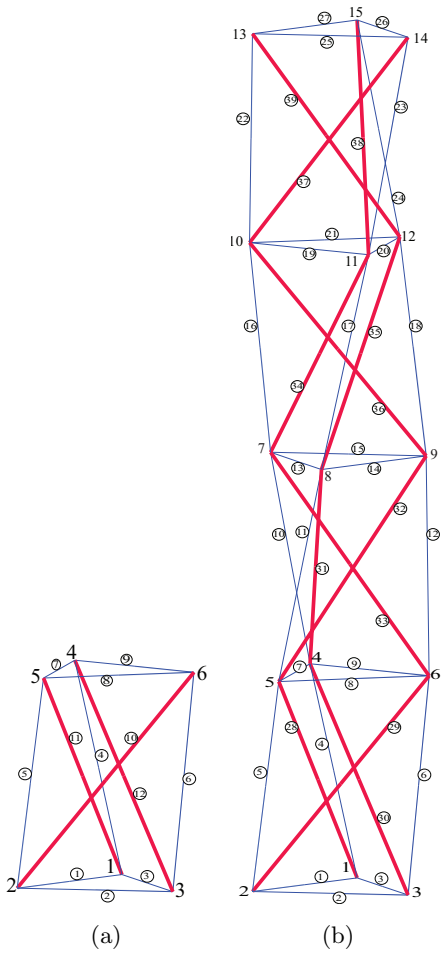

Fig. 2 Topology and the numbering scheme of, (a) The base module of T-3 tensegrity (b) Four-module T-3 tensegrity structure.

cables and compression for bars) are satisfied, for a correct design. The self-stress vector $\boldsymbol{s}_j$ of each individual module j is then seen as a scaling of the unit self-stress vector of the base module $\boldsymbol{s}_j = a_j \hat{\boldsymbol{s}}$, where a_j are the scaling factors for modules $j = 1, 2, \cdots$. The number of scaling factors equals the number of modules n.

According to the application or design requirements, the scaling factors

can be decided. When several or all a_j are equal, as implicitly used in literature (grouping), [7, 8, and many others], then group members will have the same internal force magnitudes. Grouping can be manual or automated, Koohestani [9] developed an automated method for element's grouping and self-stress identification. In this study, no pre-defined grouping was adapted in finding the self-stress vector procedure. However, finding a feasible grouping could be an important parameter in the design and optimization of tensegrity structures [9].

With this method, the scaled self-stress vector $\boldsymbol{g}$ of the whole structure can be written as a function of scaling factors a_j and the unit self-stress vector of the base module $\hat{\boldsymbol{s}}$:

$$\boldsymbol{g} = \boldsymbol{g}(a_j, \hat{\boldsymbol{s}}), \tag{2}$$

where the a_j are scalers representing the level of pre-stress in each module and $\hat{\boldsymbol{s}}$ represents the force density coefficients of each component of the base module. In other words, $\hat{\boldsymbol{s}}$ represents the internal force distribution pattern in each module. It is worth noting that in Eq. (2), the g_i corresponding to the shared elements are being added to each other. With this setup the scaling factors a_j are the free optimization parameters. From construction, these are demanded to be non-negative.

3. Finite element formulation

The finite element model used in this study represents both axial and transversal frequencies of the components, as Euler-Bernoulli beam elements were used. The geometric non-linearity of tensegrity structures is

emphasised by the coupling between the axial and bending stiffnesses of the components which has been included in the tangent stiffness matrix $\boldsymbol{k}(T) = \boldsymbol{k}_E(T) + \boldsymbol{k}_G(T)$, with a linear part $\boldsymbol{k}_E$ and a geometric part $\boldsymbol{k}_G$.

The influence of temperature changes on the dynamic properties of tensegrity structures is a complex topic, as many factors are interacting in this process. These are mainly related to a thermal expansion coefficient α and the variation of the elastic modulus E. In this study, we have made some assumptions concerning the design. The final geometry and topology of the structure are known in advance, the final geometry is connected to a specific pre-stress state, i.e., components are shortened or lengthened from an unstrained length $L_i^o(T)$, introducing axial forces when brought to their design lengths. Two parameters are affected by the temperature changes, with the following assumptions:

(i) The unstrained length $L_i^o(T)$,

$$L_i^o(T) = L_i^o(T_o)[1 + \alpha\Delta T], \tag{3}$$

where $L_i^o(T_o)$ is calculated from the self-stress vector $\boldsymbol{g}$ at a reference temperature T_o, Eqs. (1) or (2). Each element in $\boldsymbol{g}$ is, $g_i = N_i/L_i^f$, [1, 10], where N_i is the axial internal force and L_i^f is the designed length of the component i (pre-defined). But $N_i = EA_i[L_i^f - L_i^o(T_o)]/L_i^o(T_o)$ with $N_i = g_i L_i^f$, from which the unstrained length $L_i^o(T_o)$ can be calculated as $L_i^o(T_o) = EA_i L_i^f/(N_i + EA_i)$. Thus, $L_i^o(T)$ at each temperature change ΔT can be found from Eq. (3).

(ii) The change of the elastic modulus E with temperature. In literature this topic has been investigated by many researchers [11–15]. In this study,

the experimental results from [14] were adopted. Therefore, it was assumed that the materials were different steel grades. The temperature dependence of the elastic modulus was thereby assumed as

$$E(T) = E_{20}(-0.000835T + 1.0167), \tag{4}$$

where E_{20} is the elastic modulus at the design temperature, $T_o = 20$ °C, and centigrade are used for temperatures.

Both $L_i^o(T)$, Eq. (3) and $E(T)$, Eq.(4), were used to evaluate the element tangent stiffness matrix $\boldsymbol{k}_T$ and to iteratively find the corresponding equilibrium state using the Newton-Raphson method [16]. The range for ΔT considered was $\Delta T_{min} = -45 \leq \Delta T \leq \Delta T_{max} = 25$ °C and $T = T_o + \Delta T$.

The linear beam element mass matrix was calculated at T_o and not modified for ΔT. More details about the finite element model used can be found in [1, 4, 17].

With the tangent stiffness and mass matrices assembled formally as $\boldsymbol{K}(T) = \sum \boldsymbol{k}(T)$ and $\boldsymbol{M} = \sum \boldsymbol{m}$, the small free undamped vibrations of a structure around the evaluated equilibrium state were obtained from the generalized eigenproblem

$$-\omega_k^2 \boldsymbol{M}\boldsymbol{\phi}_k + \boldsymbol{K}_T\boldsymbol{\phi}_k = \boldsymbol{0}, \tag{5}$$

where ω_k^2 is one of the n eigenvalues and $\boldsymbol{\phi}_k$ the corresponding eigenvector, with n the number of active degrees of freedom. The eigenvalues were ordered so that $\omega_1 \leq \omega_2 \cdots \leq \omega_n$. The spectral decomposition thereby gave n natural frequencies ω_k and the related vibration modes $\boldsymbol{\phi}_k$ of the structure at the considered equilibrium state. As the tensegrity structures normally

contain high degrees of symmetry, the resonance solutions will normally contain sets of closely situated frequencies, and possibly eigenspaces of higher dimensions [18].

4. Optimization problem

Both ψ in Eq. (1) and a_j in Eq. (2), have been found using built in functions for a genetic algorithm (GA) of Matlab[1]. We minimized the difference between the first natural frequency ω_1 at three successive points of ΔT, chosen as -45, 0 and 25 °C (equivalent to $T = -25, 20$ and 45 °C). This is because there is a high probability for the natural frequency to change in between these two points if only ΔT_{min} and ΔT_{max} are chosen because of the non-linearity of this relation. The optimization problem was formulated as:

$$\begin{aligned} &\text{minimize} \sqrt{(\omega_1^{T_1} - \omega_1^{T_2})^2 + (\omega_1^{T_2} - \omega_1^{T_3})^2} \\ &\qquad\qquad \boldsymbol{g} = \boldsymbol{g}(a_j, \hat{\boldsymbol{s}}) \quad \text{or} \quad \boldsymbol{g} = \psi \hat{\boldsymbol{g}} \\ &\text{subject to} \quad (a_j, \psi) > 0, \end{aligned} \tag{6}$$

where $\omega_1^{T_x}$ is the first natural frequency at T_x temperature, chosen between ΔT_{min} and ΔT_{max} as mentioned above.

The only constraint applied was that the level of pre-stress had to be positive. However, the level of pre-stress has to be at least enough for the stability of the structure, otherwise the tangent stiffness matrix will be singular. The tangent stiffness matrix singularity was handled by assigning a large fitness value (estimated from multiple runs) to solutions giving singu-

[1] Version 2013a, The MathWorks, Inc., Natick, U.S.A.

larity.

The performance and efficiency of a genetic algorithm depends on some basic setups and parameters, the used ones are given in Table 1. Different results in different runs were obtained when solving the optimization problem, particularly when using the second method to find the scaling factors a_j. For this reason we have run the algorithm several times. The solution given in each example is from a typical run, which we believe is converged to a global optimum.

Table 1 Genetic algorithm setup and the basic parameters used in this study.

Parameter name	Type and value
Bounds of variables	To be positive
Population (type,size)	Double vector, 50
Selection (function)	Stochastic uniform
Crossover (type,ratio)	Heuristic, default value=1.2
Mutation (function)	Adaptive feasible
Stopping criterion	The number of generation

5. Numerical Examples and results

Two examples were considered: a 2D tube and string assembly, Fig. 1, and a 3D T3 tensegrity prism, Fig. 2(b). The first method was applied for both structures, where a unit symmetric self-stress vector was used with the level of pre-stress ψ as free parameter for the optimization problem. For the second method, only the 3D T3 tensegrity prism was considered, where an asymmetric self-stress vector was used and the level of pre-stress in each module was regulated through a_j, which are the free parameters of the optimization problem in the second method.

The focus here was to maintain the first natural frequency approximately

the same as its value f_{20}, the natural frequency at $\Delta T = 0$ ($T = 20$). In the presented Figures, the first four natural frequencies f_T at temperature T were normalized to their values f_{20}.

Tensegrity structures components can be made from same or different materials. Because of different mechanical properties requirements of tension and compression components, normally different materials for cables and bars are used. Hence, we have investigated the case when different materials are used for bars and cables. In each method, two material combinations were used. The first one was: $\rho = 7585$ kg/m^3, $\alpha_c = 9 \times 10^{-6}/^{\circ}$C and $E_{20} = 190$ GPa, for cables, and $\rho = 7585$ kg/m^3, $\alpha_b = 11.5 \times 10^{-6}/^{\circ}$C and $E_{20} = 210$ GPa, for bars. In the second material combination, we switched the material between cables and bars, and investigated the cases; $\alpha_{cable} < \alpha_{bar}$ and $\alpha_{cable} > \alpha_{bar}$.

5.1. Example 1, a tube and cable assembly

The assembly in Fig. 1 was composed of a massive circular cable with a diameter of 0.015 m and a tube (representing the bar action in a tensegrity structure) with thickness of 0.001 m and an outside diameter of 0.05 m with a designed length of 1 m. Only the first method will be adapted in this example, where the level of pre-stress will be regulated through the scaler ψ. The unique unit self-stress vector for this assembly is $\hat{\boldsymbol{g}} = [0.7071 \ -0.7071]^T$ with the cable as component 1. With a level of pre-stress of $\psi = 40$ kN/m, the first natural frequency is affected by temperature changes for both material combinations, as shown in Figs. 3(a), 3(b). For the first material combination ($\alpha_{cable} < \alpha_{bar}$), the optimum solution was found at $\psi = 37.56$ kN/m. When using the second material combination ($\alpha_{cable} > \alpha_{bar}$) the optimum solution was found to be at $\psi = 59.65$ kN/m, Figs. 4(a),

4(b).

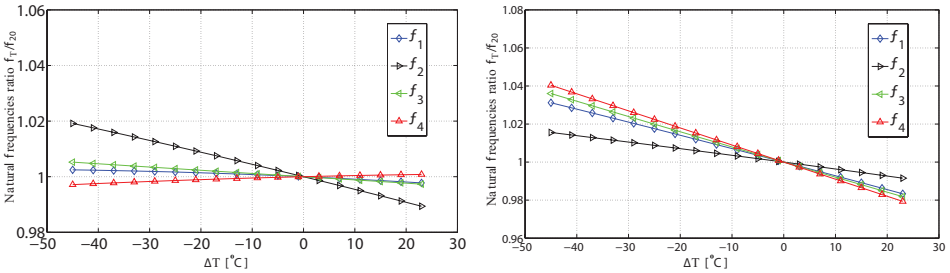

(a) $\alpha_c<\alpha_b$ (b) $\alpha_c>\alpha_b$

Fig. 3 The change of the lowest natural frequencies of the assembly shown in Fig. 1, with different relations for α coefficients and pre-decided level of pre-stress of 40 kN/m.

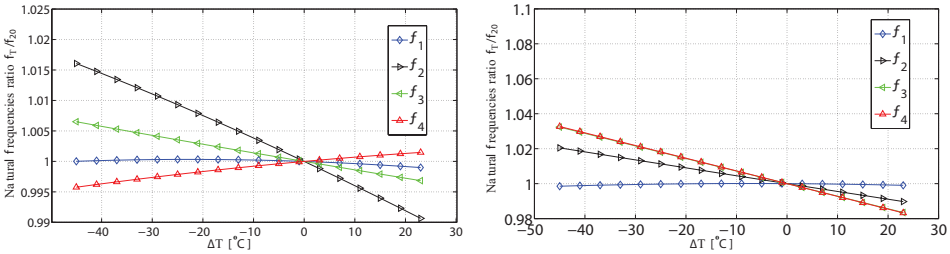

(a) $\alpha_c<\alpha_b$ with level of pre-stress of 37.56 kN/m (b) $\alpha_c>\alpha_b$ with level of pre-stress of 59.65 kN/m

Fig. 4 Optimum design of the assembly shown in Fig. 1, with different relations for α coefficients and optimum level of pre-stress, the first natural frequency is approximately constant with temperature change.

5.2. Example 2, a 3-D four-module T-3 tensegrity prism

The 3D T3 tensegrity prism, Fig. 2(b), was made up of 12 bars and 27 cables. Its nodal coordinates are listed in Table 2. All bars and cables used in the simulation were massively circular with diameters of 0.065 m and 0.015 m, respectively. For support conditions we assumed node 1 as completely fixed, node 2 as fixed in the Y and Z directions and node 3 as fixed in the Z direction.

Table 2 Nodal coordinates of the tensegrity structure shown in Fig. 2(b).

	Coordinates [m]		
Node No.	X	Y	Z
1	0.50	0.00	0.00
2	-0.25	0.433	0.00
3	-0.25	-0.433	0.00
4	0.433	0.25	2.00
5	-0.433	0.25	2.00
6	0.00	-0.50	2.00
7	0.25	0.433	4.00
8	-0.50	0.00	4.00
9	0.25	-0.43	4.00
10	0.00	0.50	6.00
11	-0.433	-0.25	6.00
12	0.433	-0.25	6.00
13	-0.25	0.433	8.00
14	-0.25	-0.433	8.00
15	0.50	0.00	8.00

Table 3 Force density coefficients of the base module and the whole structure in Fig. 2 (symmetric self-stress)

Component	Base module ($\hat{\boldsymbol{s}}$)	Whole structure ($\hat{\boldsymbol{g}}$), optimum at relevant ψ, depends on the material combination used
All side cables	0.3778	0.1853
All bars	-0.4160	-0.2040
All cables forming triangles between modules	—	0.0919
All cables forming top and bottom triangles	0.0937	0.0459

In the first method, a feasible symmetric self-stress vector $\boldsymbol{g}$ of the whole structure was found using, Eq. 2, with all $a_j = 1$ and the unit self-stress vector of the base module $\hat{\boldsymbol{s}}$ from Table 3, which was calculated from the SVD of $\boldsymbol{A}$ of the base module as in [7, 19, 20]. Values corresponding to the

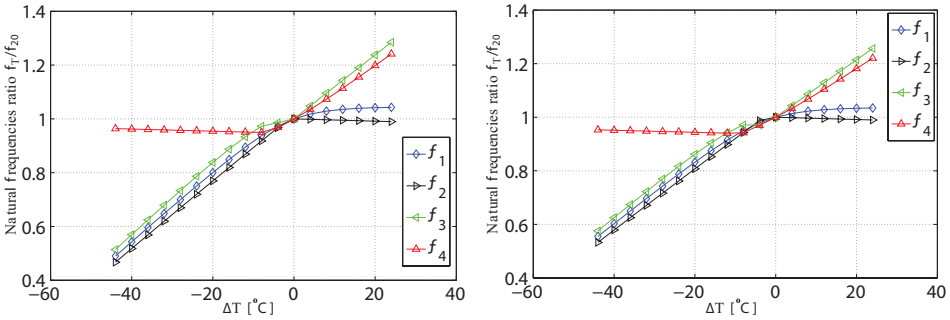

(a) $\alpha_c < \alpha_b$ with level of pre-stress of 0.55 MN/m (b) $\alpha_c > \alpha_b$ with level of pre-stress of 0.55 MN/m

Fig. 5 Non-optimum design of the T3 tensegrity structure shown in Fig. 2(b), the first natural frequency changes with temperature change.

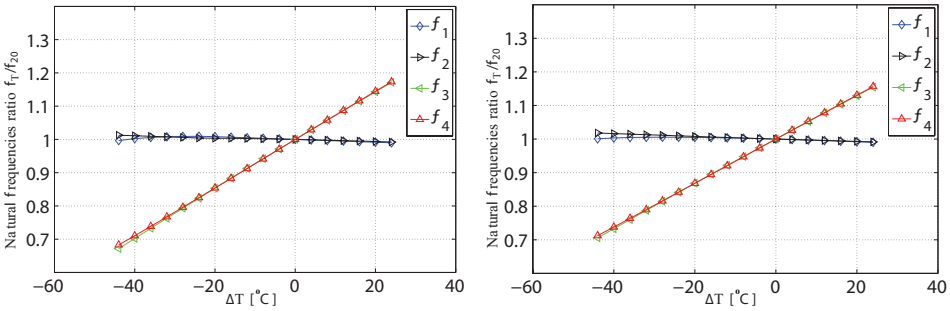

(a) $\alpha_c < \alpha_b$ with level of pre-stress of 0.881 MN/m (b) $\alpha_c > \alpha_b$ with level of pre-stress of 0.881 MN/m

Fig. 6 Optimum design of the T3 tensegrity structure shown in Fig. 2(b), using the unit self-stress vector $\hat{\boldsymbol{g}}$ from Table 3, and regulating the pre-stress level.

shared components between modules were added. Then, the unit self stress vector $\hat{\boldsymbol{g}}$ was calculated by taking the norm of $\boldsymbol{g}$.

An example for non-optimal solution is when $\psi = 0.55$ MN/m for both cases $\alpha_{cable} < \alpha_{bar}$ and $\alpha_{cable} > \alpha_{bar}$, Figs. 5(a) and 5(b), respectively. In both cases the first natural frequency changed with ΔT. It is interesting to observe that for both material combinations the optimum design was found at $\psi = 0.881$ MN/m, Figs. 6(a) and 6(b) using the same self-stress vector

Table 4 Details of the optimum self-stress values of the whole structure in Fig. 2(b)

Component #	$g_i \times 10^5$ N/m	$g_i \times 10^5$ N/m
	$\alpha_{Cable} > \alpha_{Bar}$	$\alpha_{Cable} < \alpha_{Bar}$
1-3	0.438	0.423
4-6	1.766	1.707
7-9	0.787	0.821
10-12	1.407	1.604
13-15	0.658	0.683
16-18	1.246	1.152
19-21	0.529	0.494
22-24	0.889	0.843
25-27	0.220	0.209
28-30	-1.946	-1.880
31-33	-1.550	-1.767
34-36	-1.373	-1.269
37-39	-0.980	-0.292

$\boldsymbol{g}$.

In the second method, the unit self-stress vector $\hat{\boldsymbol{s}}$ of the base module

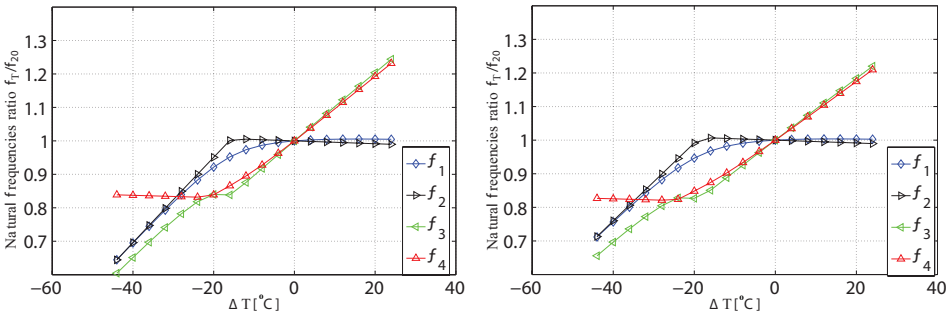

(a) $\alpha_c < \alpha_b$ (b) $\alpha_c > \alpha_b$

Fig. 7 Non-optimum design of the T3 tensegrity structure shown in Fig. 2(b), with $\hat{\boldsymbol{s}}$ from Table 3 and all $a_j = 1.3 \times 10^5$ N/m, the first natural frequency affected by temperature changes.

is given in Table 3 (found from the SVD of its equilibrium matrix $\boldsymbol{A}$). this was used to construct the self-stress vector $\boldsymbol{g}$ of the whole structure, Eq. (2). It is worth mentioning that $\boldsymbol{g}$ in this case is asymmetric, not a unit

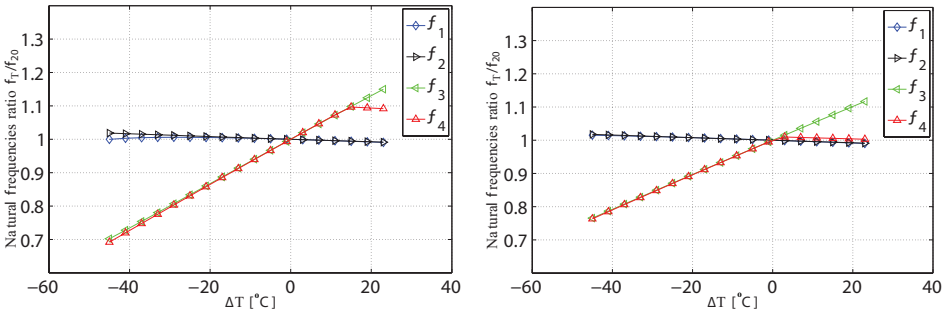

(a) $\alpha_c < \alpha_b$ (b) $\alpha_c > \alpha_b$

Fig. 8 Optimum design of the T3 tensegrity structure shown in Fig. 2(b), with the asymmetric $\boldsymbol{g}$ (not a unit vector) from Table 4, the first natural frequency is approximately constant with temperature change.

vector and it includes both the force distribution pattern and the level of pre-stress in each module. The level of pre-stress in each module j was regulated through the factors a_j (the free optimization variables in this method). Using a symmetric self-stress vector could lead to the situation where the natural frequency is affected by the temperature changes. An example for this is when all $a_j = 1.3 \times 10^5$ N/m are used, Figs. 7(a) and 7(b). The optimum solution for the case $\alpha_{cable} > \alpha_{bar}$ is found at $a_j = [1.946\ 1.550\ 1.373\ 0.980] \times 10^5$ N/m, which gives an optimum $\boldsymbol{g}$ as in Table 4. For the other case, $\alpha_{cable} < \alpha_{bar}$, the optimum self-stress vector was found at $a_j = [1.880\ 1.767\ 1.296\ 0.929] \times 10^5$ N/m, Table 4. For both material combinations used, results are shown in Figs. 8(a) and 8(b). The first natural frequency is obviously very little sensitive to the temperature changes.

6. Conclusions

It is shown that tensegrity structures can be designed such that some of their natural frequencies are little sensitive to the temperature changes.

The results from this study can be summarised in the following points:

- An asymmetric self-stress vector of a tensegrity structure can be chosen such that some of its low natural frequencies are not sensitive to the temperature changes.
- The level of pre-stress combined with a unit self-stress vector can also be used to achieve the same result above.

References

[1] Ashwear N, Eriksson A. Natural frequencies describe the pre-stress in tensegrity structures. *Computers and Structures* 2014;**138**:162–171.

[2] Guechaichia A, Trendafilova I. A simple method for enhanced vibration-based structural health monitoring. *Journal of Physics: Conference Series* 2011;**305**(1):012073.

[3] Moser P, Moaveni B. Environmental effects on the identified natural frequencies of the dowling hall footbridge. *Mechanical Systems and Signal Processing* 2011;**25**(7):2336–2357. doi:10.1016/j.ymssp.2011.03.005.

[4] Ashwear N, Eriksson A. Influence of temperature on the vibration properties of tensegrity structures. *International Journal of Mechanical Sciences* 2015;**99**:237–250.

[5] Xia Y, Chen B, Weng S, Ni Y, Xu Y. Temperature effect on vibration properties of civil structures: A literature review and case studies. *Journal of Civil Structural Health Monitoring* 2012;**2**(1):29–46.

[6] Barbosa H, Bernardino H, Angelo J. Derivative-free techniques for multiobjective structural optimization: A review. In: *Computational*

technology reviews; vol. 12. Sax-Coburg Publications Stirlingshire, Scotland; 2015, p. 27–52.

[7] Tran HC, Lee J. Initial self-stress design of tensegrity grid structures. *Computers and Structures* 2010;**88**(9-10):558–566.

[8] Tran HC, Lee J. Self-stress design of tensegrity grid structures with exostresses. *International Journal of Solids and Structures* 2010; **47**(20):2660–2671.

[9] Koohestani K. Automated element grouping and self-stress identification of tensegrities. *Engineering Computations* 2015;**32**(6):1643–1660.

[10] Vassart N, Motro R. Multiparametered form findng method: Application to tensegrity systems. *International Journal of Space Structures* 1999;**14**(2):147–154.

[11] Yan A, Kerschen G, De Boe P, Golinval J. Structural damage diagnosis under varying environmental conditions Part II: Local PCA for nonlinear cases. *Mechanical Systems and Signal Processing* 2005;**19**(4):865–880.

[12] Giraldo DF, Dyke SJ, Caicedo JM. Damage detection accommodating varying environmental conditions. *Structural Health Monitoring* 2006; **5**(2):155–172.

[13] Ancas AD, Gorbănescu D. Theoretical models in the study of temperature effect on steel mechanical properties. *Bulletin of the Polytechnic Institute of Jassy, Constructions, Architechture Section* 2006;**LII (LVI)**(1-2):49–54.

[14] Kankanamge ND, Mahendran M. Mechanical properties of cold-formed steels at elevated temperatures. *Thin-Walled Structures* 2011;**49**(1):26 – 44.

[15] Meruane V, Heylen W. Structural damage assessment under varying temperature conditions. *Structural Health Monitoring* 2012;**11**(3):345–357.

[16] Eriksson A. Equilibrium subsets for multi-parametric structural analysis. *Computer Methods in Applied Mechanics and Engineering* 1997; **140**(3-4):305–327.

[17] Ashwear N, Tamadapu G, Eriksson A. Optimization of modular tensegrity structures for high stiffness and frequency separation requirements. *International Journal of Solids and Structures* 2016;**80**:297–309.

[18] Strang G. *Linear Algebra and Its Applications*. Thomson Learning, United States of America; 1988. Third Edition.

[19] Schek H-J. The force density method for form finding and computation of general networks. *Computer Methods in Applied Mechanics and Engineering* 1974;**3**(1):115–134.

[20] Tran H, Lee J. Advanced form-finding for cable-strut structures. *International Journal of Solids and Structures* 2010;**47**(14-15):1785–1794.